High Resolution Range Profiling for Stepped Radar via Sparsity Exploitation

P. Addabbo, *Member, IEEE*, A. Aubry, *Senior Member, IEEE*, A. De Maio, *Fellow, IEEE*, L. Pallotta, *Member, IEEE*, and S.L. Ullo, *Member, IEEE*

***Abstract*—A Sparse Learning via Iterative Minimization (SLIM) approach is here used for the High Range Resolution (HRR) profile reconstruction. Stepped Frequency (SF) waveforms are also used, to achieve high range resolution while maintaining a narrow instantaneous bandwidth. The SLIM based procedure includes the Bayesian Information Criterion (BIC), for selecting active scatterers in a sparse scenario, as well as, for making the procedure as much as possible user parameter free. The carried out analysis shows that the SLIM based procedure presents higher accuracy in the HRR profile recovery when compared to other widely used techniques, i.e. the Iterative Adaptive Approach (IAA).**

***Index Terms*—High Resolution Range Profile, Stepped Frequency Radar, Cognition, Sparse Learning.**

I. Introduction

Automatic Target Recognition (ATR) [1], [2], namely the capability of a radar system to identify and characterize targets, has attracted the attention of many researchers during the last years [2]–[4]. High Range Resolution (HRR) profiling [5], [6], i.e., a one-dimensional measurement of target radar reflectivity along the slant range direction with respect to a certain radar line-of-sight (LOS) plays an important role in ATR. Unfortunately, a large instantaneous bandwidth is necessary to achieve high range resolution, representing a limiting factor from a practical point of view.

A valuable mean to overcome this drawback is provided by the Stepped Frequency (SF) technique which comprises a probing waveform strategy allowing to achieve wide or ultra-wide bandwidth, while maintaining a narrow instantaneous receiver bandwidth, easing the A/D sampling requirements, and reducing system complexity and cost [1]. In the SF approach, a series of narrowband pulses, which are stepped in frequency, is transmitted. There are several frequency hopping patterns that can be selected and the most popular assumes a linear law.

Several algorithms for estimating the unknown model parameters related to the target range profile have received significant attention in radar signal processing. Among them, the most common and widely used approaches are the matched filter, the Iterative Adaptive Approach (IAA) [7], [8], and the Sparse Learning via Iterative Minimization (SLIM) [9]. The main advantages of SLIM are a higher computational efficiency due to the use of the Conjugate Gradient Least Square (CGLS) algorithm, and fewer measurements necessary to give sparser and more accurate estimates [9].

In this work, a SLIM based procedure for HRR profile reconstruction is considered to capitalize on the HRRP sparsity. The main aspects of the method are that:

1) it resorts to the Regularized Maximum Likelihood (RML) estimation paradigm including a term promoting the sparsity of the profile that is related to the l_q-norm of the vector containing the scatterers reflectivities; a-priori information on interference power level is also accounted for at the design stage;
2) under the assumption that each range cell under test contains at most one scatterer, the actual active scatterers composing the target are determined exploiting the Bayesian Information Criterion (BIC) [10]–[12]; BIC is also used to automatic select the optimized q, so as to make the procedure as much as possible user parameter free.

Notation: We adopt the notation of using boldface lower case for vectors ($\mathbf{a}$) and boldface upper case for matrices ($\mathbf{A}$). $\mathbb{C}^N$ indicates the set of complex column vectors of length N and $\mathbb{C}^{N\times K}$ denotes the set of $N \times K$ complex matrices; $\boldsymbol{I}$ represents the identity matrix, $\mathbf{diag}\,(\boldsymbol{a})$ indicates the diagonal matrix whose i-th diagonal element is the i-th entry of $\boldsymbol{a}$ and $\mathrm{tr}\,\{\boldsymbol{A}\}$ represents the trace of the matrix $\boldsymbol{A}$. The transpose and the conjugate transpose operators are denoted by the symbols $(\cdot)^T$ and $(\cdot)^\dagger$, respectively. $\|\cdot\|$ is the Euclidean norm of the argument. $\mathbb{E}[\cdot]$ denotes the statistical expectation. Finally, the letter j represents the imaginary unit (i.e., $j=\sqrt{-1}$).

II. Signal Model

A coherent monostatic radar system is considered which transmits a train of N frequency modulated pulses of duration T_p and Pulse Repetition Interval (PRI) T, with $T_p < T$. The n-th transmitted pulse, with $n = 1, \ldots, N$, can be expressed as

$$s(n,t) = \frac{\sqrt{P}}{\sqrt{T_p}}\mathrm{rect}\left(\frac{t-(n-1)T-T_p/2}{T_p}\right)e^{j2\pi f_n(t-(n-1)T)} \tag{1}$$

where:

- P is the radar transmit peak power;

Pia Addabbo is with the Università Telematica "Giustino Fortunato", 82100, Benevento, Italy. E-mail: p.addabbo@unifortunato.eu.

Augusto Aubry and Antonio De Maio are with the Università degli Studi di Napoli "Federico II", Dipartimento di Ingegneria Elettrica e delle Tecnologie dell'Informazione, Via Claudio 21, I-80125 Napoli, Italy. E-mail: augusto.aubry@unina.it, ademaio@unina.it.

Luca Pallotta is with CNIT udr Università "Federico II", via Claudio 21, I-80125 Napoli, Italy. E-mail: luca.pallotta@unina.it.

S.L. Ullo is with the the Università degli Studi del Sannio, Dipartimento di Ingegneria, Piazza Roma 21, 82100 Benevento, Italy. E-mail: silvullo@unisannio.it.

- $\text{rect}(\tau)$ is the rectangular window, that is equal to 1 as $-0.5 \leq \tau \leq 0.5$, and 0, otherwise;
- $f_n = f_c + c_n\beta/2$, is the n-th transmitted frequency belonging to a discrete set, with $c_n \in [-1, 1]$.

The vector $\mathbf{c} = [c_1, c_2, \ldots, c_N]^T$ defines the frequency hopping pattern and is referred to as frequency modulation code.

The signal at the receiver, after down-conversion and filtering operation, is sampled at fast-time instants $t_s(n-1, l_r)$, with l_r indicating a coarse range cell. The discrete-time echo signal from the $k-$th stationary scatter located at the range r_k can be expressed as (under some mild technical conditions) [13]

$$y_k(n, t_s(n-1, l_r)) = \bar{\gamma_k}\sqrt{P}e^{j\zeta_k c_n} \tag{2}$$

where:

- $\bar{\gamma_k} = \gamma_k \exp(j4\pi f_c R_k/c)$,
- $\zeta_k = 2\pi\beta R_k/c$,

with $R_k = r_s(l_r) - r_k$, the high-resolution range displacement of the scatterer from the processed coarse range bin position, and γ_k, the corresponding scattering coefficient.

Accounting for the presence of the K scatterers, within the coarse range bin associated with l_r, and considering the noise contribution, the signal model, in vector notation, can be expressed as

$$\boldsymbol{y} = \sqrt{P}\,\boldsymbol{H}(\boldsymbol{r}, \boldsymbol{c})\bar{\boldsymbol{\gamma}} + \boldsymbol{n}, \tag{3}$$

where

- $\boldsymbol{r} = [R_1, \ldots, R_K]^T \in [0, cT_p/2]^K$ is the vector containing the HRR displacements;
- $\bar{\boldsymbol{\gamma}} = [\bar{\gamma}_1, \ldots, \bar{\gamma}_K]^T \in \mathbb{C}^K$ is the vector containing the reflectivities of the scatterers within the coarse range bin under test;
- $\boldsymbol{n} \in \mathbb{C}^N$ denotes the received disturbance signal, modeled as a zero mean, white, complex circularly symmetric Gaussian random vector.

The model matrix $\boldsymbol{H}(\boldsymbol{r}, \boldsymbol{c}) \in \mathbb{C}^{N\times K}$ is defined as

$$\boldsymbol{H}(\boldsymbol{r}, \boldsymbol{c}) = [\boldsymbol{h}(R_1, \boldsymbol{c}), \boldsymbol{h}(R_2, \boldsymbol{c}), \ldots, \boldsymbol{h}(R_K, \boldsymbol{c})], \tag{4}$$

with

$$\boldsymbol{h}(R, \boldsymbol{c}) = \left[e^{j2\pi\frac{\beta}{c}R\,c_1}, \ldots, e^{j2\pi\frac{\beta}{c}R\,c_N}\right]^T \in \mathbb{C}^N,$$

the normalized response of a scatterer located at the range increment R (target steering vector).

III. HRRP VIA SLIM

In this section, a HRR profile recovery strategy based on SLIM [9] is discussed. To this end, let $\bar{R}_1, \bar{R}_2, \ldots, \bar{R}_{K_1}$ be a discrete set of possible range increments such that $\{R_1, R_2, \ldots, R_K\} \subseteq \{\bar{R}_i\}_{i=1}^{K_1}$. Under this assumption, the signal model (3), can be expressed as

$$\boldsymbol{y} = \boldsymbol{A}\boldsymbol{x} + \boldsymbol{n}, \tag{5}$$

with the model matrix defined as

$$\boldsymbol{A} = \sqrt{P}[\boldsymbol{h}(\bar{R}_1, \boldsymbol{c})\boldsymbol{h}(\bar{R}_2, \boldsymbol{c}), ..., \boldsymbol{h}(\bar{R}_{K_1}, \boldsymbol{c})]$$

and the hypothesis that the number of measurements N is smaller than unknowns K_1 and the signal vector $\boldsymbol{x} = [x_1, \ldots, x_{K_1}]^T$ has most of its elements equal to 0, i.e., it is sparse. Under these hypotheses, that are valid for many radar applications in which the scene is essentially sparse, the problem in (5) can be solved via SLIM, recovering both the sparse signal and the noise power, which is not always a-priori available.

The regularized minimization problem for the sparse signal reconstruction can be formulated as

$$\mathcal{P}\begin{cases} \min\limits_{\bar{\boldsymbol{\gamma}}, \sigma^2} & N\log(\sigma^2) + \frac{1}{\sigma^2}\|\boldsymbol{y} - \boldsymbol{A}\boldsymbol{x}\|^2 + f_q(\boldsymbol{x}) \\ \text{s.t.} & \sigma_L^2 \leq \sigma^2 \leq \sigma_U^2 \end{cases} \tag{6}$$

where

$$f_q(\boldsymbol{x}) = \sum_{k=1}^{K_1}\frac{2}{q}\left[\left(|x_k|^2 + \epsilon\right)^{q/2} - 1\right] \tag{7}$$

is the sparsity promoting penalty term, with $\epsilon > 0$ a smoothing factor making (7) differentiable. In (6), σ_L^2 and σ_U^2 are respectively a lower bound and an upper bound to the noise power, where σ_L^2 can be evaluated characterizing the power level associated with the isolated operation of the receiver components, whereas σ_U^2 can be obtained exploiting some a-priori information and previous measurements.

It is worth pointing out that the regularized minimization problem $\mathcal{P}$ is on the same line as the recovery approach developed in [9]. If the initial estimates of $\boldsymbol{x}$ and σ^2 are given, e.g. via a matched filtering, it is possible to apply a cyclic optimization procedure, which can be defined as in the Algorithm 1.

Algorithm 1 SLIM for HRR profiling

1: **Input.** σ_L^2, σ_U^2, $\epsilon > 0$, $\Delta > 0$, and $q \in [0, 1]$.
2: **Initialization.** Set $t = 0$, $\sigma^{2^{(0)}} = \sigma_L^2$, and $x_i^{(0)} = \boldsymbol{h}_i^\dagger \boldsymbol{y}/\sqrt{P}$, $i = 1, \ldots, K_1$, with $\boldsymbol{h}_i = \boldsymbol{h}(\bar{R}_i, \boldsymbol{c})/||\boldsymbol{h}(\bar{R}_i, \boldsymbol{c})||^2$.
3: **repeat**
4: $t = t + 1$
5: $\boldsymbol{B}^{(t-1)} = \mathbf{diag}\,(\boldsymbol{b}^{(t-1)} + \epsilon)$, with $\boldsymbol{b}^{(t-1)} = \left[|x_1^{(t-1)}|^{2-q}, |x_2^{(t-1)}|^{2-q}, ..., |x_{K_1}^{(t-1)}|^{2-q}\right]^T$
6: $\boldsymbol{x}^{(t)} = \boldsymbol{B}^{(t-1)}\boldsymbol{A}^\dagger\left(\boldsymbol{A}\boldsymbol{B}^{(t-1)}\boldsymbol{A}^\dagger + \sigma^{2^{(t-1)}}\boldsymbol{I}\right)^{-1}\boldsymbol{y}$
7: $\sigma^{2^{(t)}} = \min\left(\max\left(\sigma_L^2, \hat{\sigma}^2\right), \sigma_U^2\right)$ with $\hat{\sigma}^2 = \frac{1}{N}\|\boldsymbol{y} - \boldsymbol{A}\boldsymbol{x}^{(t)}\|_2^2$
8: **until** $\|\boldsymbol{x}^{(t)} - \boldsymbol{x}^{(t-1)}\|_2/\|\boldsymbol{x}^{(t)}\|_2 < \Delta$
9: **Output.** Estimated profile $\hat{\boldsymbol{x}}$.

In the following subsections, the estimated profile form Algorithm 1 is used as input for the successive steps of the proposed method:

1) the selection of active scatterers;
2) the HRR reconstruction via Least Square (LS) on the selected scatterers;
3) the automatically estimation of q.

A. BIC for active scatterers

In this subsection, the coarse range cell of interest is divided in N_c disjoint range cells, and each cell is discretized with $M_s > 1$ sub-bins. The range increments subset

$$\mathcal{A}_i = \{R_{1+(i-1)M_s}, \ldots, R_{M_s+(i-1)M_s}\}$$

is associated to the i-th cell with $i = 1, \ldots, N_c$. Hence, the overall range increment set is given by $\mathcal{A} = \cup_{i=1}^{N_c} \mathcal{A}_i = \left\{\bar{R}_1, \bar{R}_2, \ldots, \bar{R}_{K_1}\right\}$, with $K_1 = N_c M_s$.

Under the hypothesis that at most one scatterer is contained in each cell, a BIC-based strategy is performed for selecting the number of active scatterers.

Given $\boldsymbol{x}^{\bar{q}}$ the SLIM estimate from Algorithm 1, with $q = \bar{q}$, applied to the steering vectors associated with $\mathcal{A}$, let $\bar{K}$, an upper bound to the actual number of scatterers and $\mathcal{I}(k) = \{\tilde{i}_1^\star, \ldots, \tilde{i}_{k-1}^\star\}$, the set of the selected $k-1$ scatterer indices at iteration $k-1$.

Then, at step k, the sub-range index of the selected scatterer is found as

$$\tilde{i}_k^\star = \arg \min_{\tilde{i} \notin \cup_{h \in \mathcal{I}(k)}^{k-1} \mathcal{A}_h} \mathrm{BIC}_k^{\bar{q}}(\tilde{i}) \tag{8}$$

with

$$\mathrm{BIC}_k^{\bar{q}}(\tilde{i}) = 2N \log \left(\|\boldsymbol{y} - \sum_{i \in \left\{\mathcal{I}(k) \cup \{\tilde{i}\}\right\}} \boldsymbol{a}_i \hat{x}_i{}^{\bar{q}} \|^2 \right) + 3k \log(2N), \; k = 1, \ldots, \bar{K}, \tag{9}$$

where the factor 3, in the second term, represents the number of unknowns for each source, i.e., the complex valued amplitude and its position, $\boldsymbol{a}_i$ is the i-th column of the matrix $\boldsymbol{A}$ and $x_i{}^{\bar{q}}$ is the i-th element of $\hat{\boldsymbol{x}}^{\bar{q}}$. Remarkably, the constraint $\tilde{i} \notin \cup_{h \in \mathcal{I}(k)}^{k-1} \mathcal{A}_h$ in Equation (9) inhibits the choice of a sub-bin lying in a range cell already occupied by a previously selected scatterer. In other words, at the $k-$th iteration of the algorithm a new scatterer (lying in a range cell different from that of the scatterers composing the range profile estimate optimized up to step $k-1$) is selected such that the updated range profile minimizes (9) and this procedure is repeated until $k \leq \bar{K}$. Hence, denoting by

$$k^\star = \arg \min_{k \in \{1, \bar{K}\}} \mathrm{BIC}_k^{\bar{q}}(\tilde{i}_k^\star), \tag{10}$$

the RP recovery is obtained from $\mathcal{I}(k^\star)$.

B. LS amplitudes

Let $\boldsymbol{A}_o^{\bar{q}}$ be the model matrix obtained extracting from the entire model matrix only the columns corresponding to the active scatterers selected using the procedure explained in Section III-A, with $q = \bar{q}$. Thus, for each selected sub-bin position (non-selected positions have a zero amplitude value), the final values of $\hat{\boldsymbol{x}}_R^{\bar{q}}$ is computed via the least-squares estimate on the active scatterers as

$$\hat{x}_R^{\bar{q}}(i) = \begin{cases} \left(\boldsymbol{A}_o^{\bar{q}T} \boldsymbol{A}_o^{\bar{q}}\right)^{-1} \boldsymbol{A}_o^{\bar{q}T} \boldsymbol{y}, & \text{if } i \in \mathcal{I}(k^\star) \\ 0, & \text{otherwise.} \end{cases} \tag{11}$$

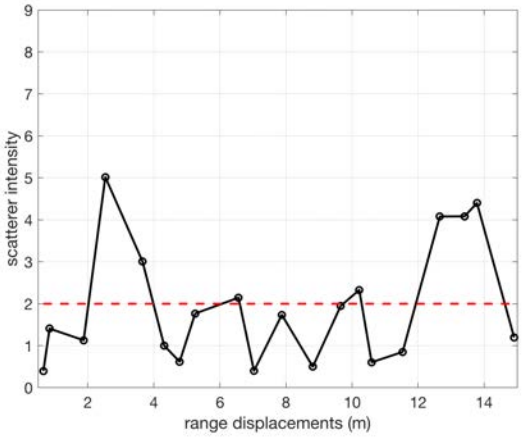

Fig. 1. Modulus of the realistic sparse profile used for simulation.

C. Adaptive Selection on q

Here, again, a model order selection is used to make the proposed procedure as much as possible user parameter free [11]. To this end, a BIC approach to evaluate q is used, but it can easily be extended to also account for the other parameters, such as the smoothing factor ϵ.

Denoting by $\mathcal{I}_q \subseteq (0, 1]$ the discrete set of the considered q values, the selection is done using the BIC criterion

$$q^\star = \arg \min_{q \in \mathcal{I}_q} \mathrm{BIC}(q), \tag{12}$$

with the objective function defined as

$$\mathrm{BIC}(q) = 2N \log\left(\|\boldsymbol{y} - \boldsymbol{A}\boldsymbol{x}_R^q\|^2\right) + 3h(q) \log(2N), \tag{13}$$

where $\boldsymbol{x}_R^q$ represents the profile estimate resulting from SLIM with both BIC for active scatterers selection and LS amplitudes estimation, for a given q, whereas $h(q)$ stands for the number of active sub-bins, i.e., the values of $\boldsymbol{x}_R^q$ different from zero.

IV. Performance analysis

In this section, the ability of the SLIM approach to reconstruct the HRR profile is assessed also in comparison with the IAA. To make as much as possible fair the performance comparison, the IAA estimated HRR profile is elaborated with further post-processing, namely, the selection of active scatterers and the LS estimate on the selected sub-bins.

The analysis is conducted for realistic simulated profiles that are created as follows:

- a measured profile at a nominal range resolution is considered (the black line in Figure 1);
- a range profile with dominant scatterers is constructed setting a threshold (dashed red line in Figure 1), accounting for an estimate of the interference power level (the samples below this threshold are set to zero);
- finally, the location of any detected dominant scatterer is obtained randomly generating the sub-bin within the range cell.

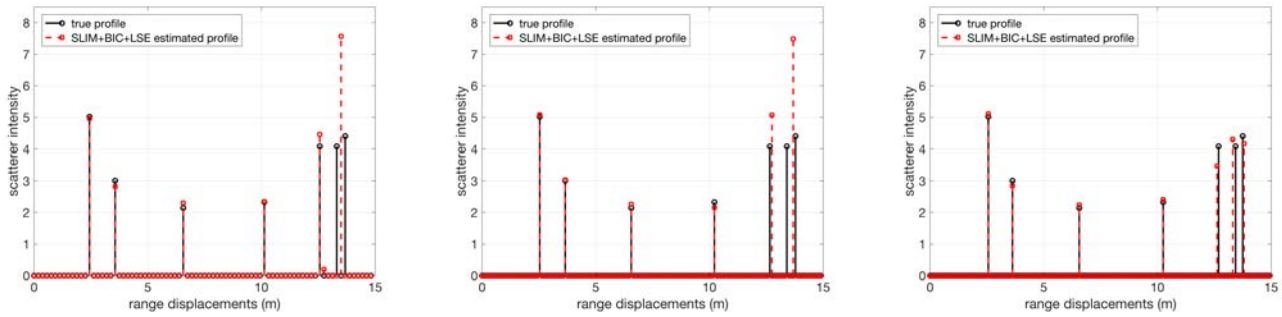

Fig. 2. Modulus of the HRR realistic profiles for a burst of $N = 36$ transmitted pulses, SNR = 1 dB, and a number of sub-bins of 4 (left), 8 (center), and 12 (right): black stems represent the true profile while dashed red ones correspond to the SLIM estimated profile.

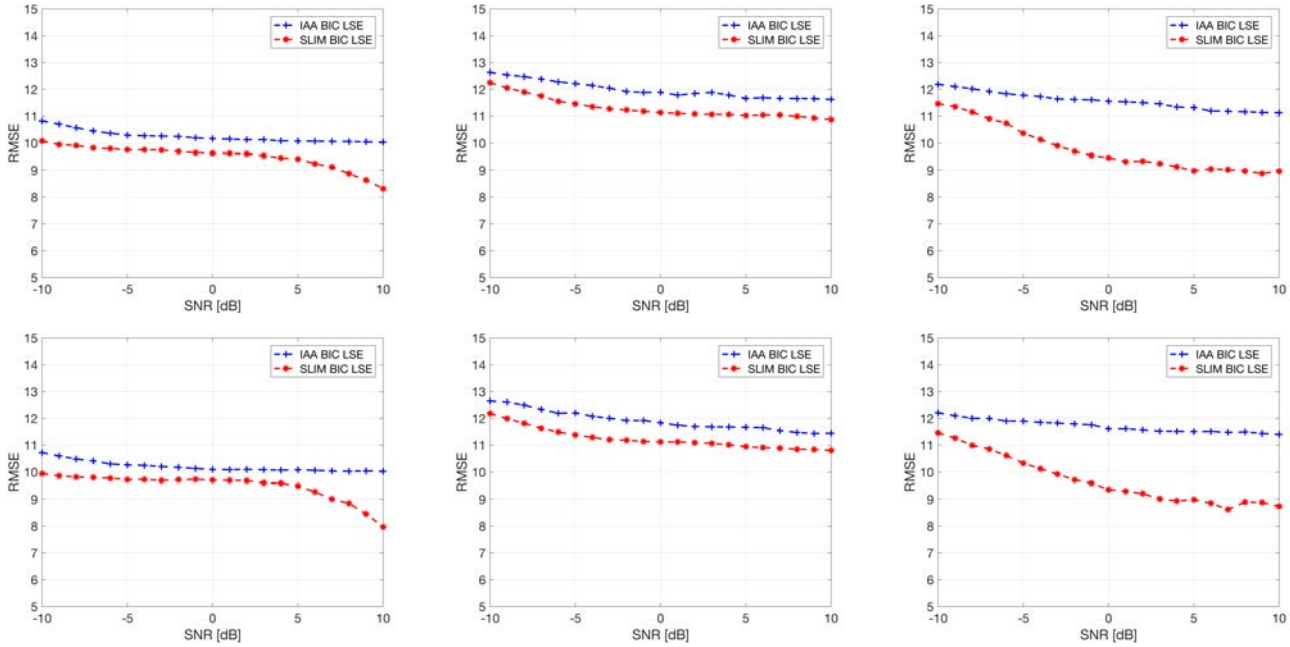

Fig. 3. Linear Stepped Frequency Performance: N = 36 in the first row, N = 40 in the second one, while the number of sub-bins is 4 on the left column, 8 at the center column, and 12 on the right column. Red curves represent the SLIM performance while blue lines the IAA.

Furthermore, in all the simulations, the following parameters have been considered:

- $\epsilon = 10^{-5}$;
- β = 200 MHz;
- f_c = 9 GHz;
- T_p = 0.1 μs;
- T = 1 μs;
- σ_L^2 is set equal to half of the true noise power;
- $\sigma_U^2 = 100$.

The phases of the complex valued scatterers are modeled as independent and identically distributed (i.i.d.) uniform random variables within $[0, 2\pi)$.

As stated above, from the realistic profile represented in Figure 1, the HRR is constructed randomly varying the position of the scatterers within the selected number of sub-bins M_s, which is fixed at 4, 8, and 12, namely at 0.1875, 0.0938, and 0.0625 m range displacements. In Figure 2, the three SLIM estimated HRR profiles (red stems) with respect to the real ones (black stems) are shown: the number of sub-bins for the high resolution is 4, on the left, 8, at the center, and 12, on the right. In this case, a burst composed of $N = 36$ linear frequency stepped pulses is considered, and a single realization of noise is added leading to a SNR of 1 dB.

The Root Mean Square Error (RMSE) of the RP is considered as figure of merit, i.e.:

$$\text{RMSE} = \sqrt{\mathbb{E}\left[\left\|\boldsymbol{x}_R - \hat{\boldsymbol{x}}_R\right\|^2\right]}, \tag{14}$$

where $\boldsymbol{x}_R$ is the vector of the true RP whose elements are the reflectivities of the scatterers associated to the sub-bins (characterized by many zeros), and $\hat{\boldsymbol{x}}_R$ is the estimated counterpart. Since the statistical expectation in (14) cannot be computed in closed form, its estimate is obtained through a number of MC simulations, set equal to 500 in the following analysis. Figure 3 shows the RMSE of the RP estimate obtained via SLIM and IAA, assuming as true RP those in Figure 2 (namely, at each MC iteration, the positions of the scatterers remain the same). Specifically, the first row plots refer to N = 36, whereas the

second row plots assume $N = 40$. Additionally, 4, 8, and 12 sub-bins are supposed in left, center, and right column plots, respectively.

The curves show that the proposed SLIM based procedure is capable of achieving better performance with respect to the IAA, ensuring a lower RMSE value for both the considered number of pulses. When a greater number of pulses ($N = 40$) is used, both the procedures obtain a gain in terms of RMSE, which is also more significant for SLIM.

V. Conclusions and future work

A procedure based on SLIM, an l_q-norm based regularized method, has been considered for HRR profile recovery. The algorithm has included the BIC model order selection, to make the procedure as much as possible user parameter free (automatically estimating q) and to select the number of the active scatterers in a sparse scenario.

The performance of the proposed algorithm has been assessed through the simulation of realistic sparse profiles at varying range sub-bin numbers. Comparisons with IAA show that SLIM achieves better results when the linear stepped pattern is used.

It is worth noticing that even in the presence of comparable performance, the SLIM based procedure, by incorporating the CGLS approach, can obtain some computational advance over IAA [9].

For future work, it could be useful to take into account that there are several frequency hopping patterns that can be selected. In fact, the most popular assumes a linear law, which possibly presents a ridge in the range-Doppler ambiguity function. A possible solution to the aforementioned problem is obtained when the transmitted frequencies are randomly changed, rather than linearly [14]. Thus, the frequency hopping pattern still represents a degree of freedom and several examples are provided in the literature [15]–[21].

References

[1] W. L. Melvin and J. A. Scheer, *Principles of Modern Radar: Advanced Techniques*, vol. 2, SciTech Publishing, 2013.

[2] P. Tait, *Introduction to Radar Target Recognition*, vol. 18, IET, 2005.

[3] A. R. Persico, C. Clemente, D. Gaglione, C. Ilioudis, J. Cao, L. Pallotta, A. De Maio, I. Proudler, and J. J. Soraghan, "On Model, Algorithms and Experiment for Micro-Doppler based Recognition of Ballistic Targets," *IEEE Transactions on Aerospace and Electronic Systems*, vol. 53, no. 3, pp. 1088–1108, June 2017.

[4] C. Clemente, L. Pallotta, D. Gaglione, A. De Maio, and J. J. Soraghan, "Automatic Target Recognition of Military Vehicles With Krawtchouk Moments," *IEEE Transactions on Aerospace and Electronic Systems*, vol. 53, no. 1, pp. 493–500, February 2017.

[5] A. Zyweck and R. E. Bogner, "Radar Target Classification of Commercial Aircraft," *IEEE Transactions on Aerospace and Electronic Systems*, vol. 32, no. 2, pp. 598–606, April 1996.

[6] M. Vespe, C. J. Baker, and H. D. Griffiths, "Radar Target Classification using Multiple Perspectives," *IET Radar, Sonar Navigation*, vol. 1, no. 4, pp. 300–307, August 2007.

[7] W. Roberts, P. Stoica, J. Li, T. Yardibi, and F. A. Sadjadi, "Iterative Adaptive Approaches to MIMO Radar Imaging," *IEEE Journal of Selected Topics in Signal Processing*, vol. 4, no. 1, pp. 5–20, 2010.

[8] S. D. Blunt, K. Gerlach, and T. Higgins, "Aspects of Radar Range Super-Resolution," in *IEEE Radar Conference*, April 2007, pp. 683–687.

[9] X. Tan, W. Roberts, J. Li, and P. Stoica, "Sparse learning via iterative minimization with application to mimo radar imaging," *IEEE Transactions on Signal Processing*, vol. 59, no. 3, pp. 1088–1101, March 2011.

[10] H. L. Van Trees, *Detection, Estimation, and Modulation Theory*, John Wiley & Sons, 2004.

[11] P. Stoica and Y. Selén, "Model-Order Selection: A Review of Information Criterion Rules," *IEEE Signal Processing Magazine*, vol. 21, no. 4, pp. 36–47, 2004.

[12] Y. Selén, *Model Selection*, Phd dissertation in electrical engineering, Uppsala University, Sweden, October 2004.

[13] A. Aubry, V. Carotenuto, A. De Maio, and L. Pallotta, "High Range Resolution Profile Estimation via a Cognitive Stepped Frequency Technique," *under review on IEEE Trans. on Aerospace and Electronic Systems*, vol. xx, no. xx, pp. xx, 2018.

[14] Y. Liu, H. Meng, G. Li, and X. Wang, "Range-velocity estimation of multiple targets in randomised stepped-frequency radar," *Electronics Letters*, vol. 44, no. 17, pp. 1032–1034, Aug 2008.

[15] J. E. Luminati, T. B. Hale, M. A. Temple, M. J. Havrilla, and M. E. Oxley, "Doppler Aliasing Artifact Filtering in SAR Imagery Using Randomised Stepped-Frequency Waveforms," *Electronics Letters*, vol. 40, no. 22, pp. 1447–1448, October 2004.

[16] S. R. J. Axelsson, "Analysis of Random Step Frequency Radar and Comparison With Experiments," *IEEE Transactions on Geoscience and Remote Sensing*, vol. 45, no. 4, pp. 890–904, 2007.

[17] T. Huang, Y. Liu, H. Meng, and X. Wang, "Cognitive Random Stepped Frequency Radar with Sparse Recovery," *IEEE Transactions on Aerospace and Electronic Systems*, vol. 50, no. 2, pp. 858–870, April 2014.

[18] C. Y. Chen and P. P. Vaidyanathan, "MIMO Radar Ambiguity Properties and Optimization Using Frequency-Hopping Waveforms," *IEEE Transactions on Signal Processing*, vol. 56, no. 12, pp. 5926–5936, December 2008.

[19] S. Gogineni and A. Nehorai, "Frequency-Hopping Code Design for MIMO Radar Estimation Using Sparse Modeling," *IEEE Transactions on Signal Processing*, vol. 60, no. 6, pp. 3022–3035, June 2012.

[20] D. Zhao and Y. Wei, "Adaptive Gradient Search for Optimal Sidelobe Design of Hopped-Frequency Waveform," *IET Radar, Sonar Navigation*, vol. 8, no. 4, pp. 282–289, April 2014.

[21] D. Zhao, Y. Wei, and Y. Liu, "Steepest Descent Method for Minimizing the Peak Sidelobe Level of Hopped-Frequency Waveform," in *2017 IEEE Radar Conference (RadarConf)*, May 2017, pp. 0586–0590.